TECHNICAL MEMORANDUM

453

African easterly jet in the ECMWF integrated forecast system: 4DVar analysis

A. M. Tompkins[1], A. Diongue[2], D. J. Parker[3] and C. D. Thorncroft[4]

Research Department

[1] ECMWF
[2] Direction de la Meteorologie Nationale, Dakar-Yoff, Senegal
[3] Institute for Atmospheric Science, University of Leeds, Leeds, UK
[4] Department of Earth and Atmospheric Science, University at Albany, New York, USA

Submitted to Q.J. Roy. Meteor. Soc.

December 2004

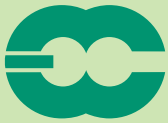

European Centre for Medium-Range Weather Forecasts
Europäisches Zentrum für mittelfristige Wettervorhersage
Centre européen pour les prévisions météorologiques à moyen terme

Series: ECMWF Technical Memoranda

A full list of ECMWF Publications can be found on our web site under:
http://www.ecmwf.int/publications/

Contact: library@ecmwf.int

European Centre for Medium-Range Weather Forecasts
Shinfield Park, Reading, RG2 9AX, England

Abstract

In August 2000, the Met Office C130 research flight aircraft conducted four sorties over the Western Sahel region, making dropsonde measurements at an unprecedented resolution. These were used as an independent validation source to assess the quality of the analysis of the African easterly jet (AEJ) in the European Centre for medium range forecasts (ECMWF) integrated forecast system. The model was found to produce a reasonably accurate representation of the AEJ location and structure. Peak zonal winds were within 5 ms^{-1} of the observed values for the two flights that performed transects across the jet. Temperature errors were less than 1K above the boundary layer, and the gross features of the humidity distribution were reproduced. The analysis was also able to capture the weak African Easterly Wave activity present during the campaign, but was not capable of reproducing the observed daily variability in boundary layer height, with a too deep mixed layer on two days resulting in a significant dipole error structure in temperature and relative humidity.

Analysis experiments were conducted in which various observations were excluded from the system to determine which were important for the diagnosis of the jet. Satellite data had a minor influence on the jet structure. Conventional platforms such as radiosondes and pilot balloons were more important. The thermodynamical information from radiosondes had a greater impact on the jet winds than the direct assimilation of the wind observations, made possible by the 4D variational assimilation system where thermodynamic information can impact the dynamics. In contrast, the jet structure improved when surface observations (synop) were removed from the system, possibly due to the disparity between the radiosonde and synop station humidity information over these regions. The investigation implied that all observational information is incorporated into the analysis in a well balanced manner, rather than being dominated by a single source. The system was able to assimilate the dropsonde data, which led to an improved dynamical and thermodynamical structure of the jet.

1 Introduction

1.1 The African easterly Jet

The African easterly jet (AEJ hereafter) is one of the key elements of the West African Monsoon (WAM) system, a major climatic feature of sub-Saharan North Africa that also has important impacts on the tropical North Atlantic (Sultan et al., 2003; Sultan and Janicot, 2003). The AEJ system, while exhibiting deceptively simple climatological structure, involves a spectrum of interacting features and physical processes (Redelsperger et al., 2002). There is a notable interplay between processes that act to maintain geostrophic balance and the combined effects of dry and moist convective regimes to the north and south respectively (Karyampudi and Carlson, 1988; Thorncroft and Blackburn, 1999). The AEJ exists in the Tropical North African mid-troposphere between March and October with a mean intensity of about 15 ms^{-1} and extends from the Red sea to the Atlantic with a meridional position varying from 10°N to 15°N, between June and August (Burpee, 1972). The lower troposphere of the West African monsoon is characterised by south-westerlies associated with the progression of the monsoon.

The AEJ plays a crucial role in the development of West African synoptic-scale and mesoscale weather systems. The positive meridional surface temperature gradient and the sign reversal of the meridional PV gradient associated with the AEJ satisfy the necessary criteria of barotropic and baroclinic instabilities, leading to the development of the synoptic African easterly waves (AEWs) at the expense of the AEJ, which modulate convection over West Africa (Fink and Reiner, 2003). The vertical wind shear associated with the AEJ promotes the organisation of mesoscale convective systems (MCSs) which produce 95 % of the rainfall in the Sahel (Laurent et al., 1998). Multi-scale numerical simulations indicate in turn that the MCSs locally intensify and deepen the AEJ after their passage due to the rear inflow and associated downdraughts (Diongue et al., 2002). The WAM and the AEJ are sensitive to meridional surface gradients of mass and energy across West Africa and these gradients are themselves sensitive to surface conditions (albedo, vegetation, soil moisture) and sur-

face and boundary layer processes (radiation, turbulence, convection) (Eltahir, 1998; Zheng and Eltahir, 1998; Zheng et al., 1999; Fontaine et al., 1999).

1.2 Analysis of the jet

Despite the importance of the AEJ in the WAM system, the actual routine network over West Africa is quite sparse. A considerable part of our present understanding derives from modelling studies, either in the form of idealized simulations, or from data assimilation systems. Considering the reliance of these model-based studies on uncertain parameterizations, it is important to assess the quality of their representation of the AEJ. In particular it is possible that the sparsity of the observational network could lead to a heavy reliance of analyses on the underlying climatology of the forecast model. Reed et al. (1988) made an evaluation of the model performance in analysing AEWs in West Africa and the tropical Atlantic, but this study was also hindered by the sparsity of *in situ* data.

The sparsity of routine observations over northern and tropical Africa is a matter of international concern. Given the limited resources of many of the African nations, it is not pragmatic simply to recommend increased resolution and frequency of upper air observations. It is necessary to recommend a sustained observing system for the region based on a knowledge of the relative merits of different data streams, be they surface, upper air or remote-sensed data. In order to address such practical issues, it is first necessary to establish the importance of different data streams within the current observing system to practical NWP and climate prediction, and secondly to attempt to evaluate the impact of possible new observations. This paper addresses the first of these questions.

1.3 The Jet2000 campaign

In order to address these issues of model evaluation and data impacts, the JET2000 experiment, which took place over West Africa during August 2000, provided unprecedented high-resolution observations in the region. Using the Met Office Met Research Flight C-130 aircraft, four flights with dropsondes involving transects along and across the AEJ were made in addition to the meridional aircraft measurements in the boundary layer. In total, 112 dropsondes were deployed at 0.5-1 degree resolution and for each flight, and the majority of the dropsonde data were assimilated in real time in the Meteorological Office (UK) and ECMWF systems. Thorncroft et al. (2003) provide a description of the logistics of the flights and some preliminary comparisons of the analyses for one flight on 28 August, showing a good representation of the AEJ.

One possible caveat on this work is the possible lack of generality of conclusions drawn from such a short timeseries of four days of measurements. Despite the broad predictability of the monsoon progression, this region exhibits marked inter and intra-seasonal variability (Le Barbé et al., 2002), and indeed, Thorncroft et al. (2003) point out that 2000 was unusual, with a dry late season and a stronger sustained jet displaced to the south (two characteristics commonly observed in tandem over this region, e.g. Nicholson, 1981; Newell and Kidson, 1984; Grist and Nicholson, 2001; Nicholson and Grist, 2003). This can be seen in fig. 1, which compares the August monthly mean operational analysis for 2000 to the 42 year August climatology of the ERA-40 reanalysis (Simmons and Gibson, 2000). The jet in the climatology is weakened by the compositing procedure, but comparison to individual years (not shown) proves that the jet is indeed stronger and more equatorwards than usual in the 2000 summer season.

On the other hand, the analysis can be (over) simplistically viewed as an interpolation of the incomplete observations representing the 'truth' (assuming no observation error), and the model climatology. If the analysis errors relative to a high quality, high resolution dataset available over a short period of time broadly reflect the

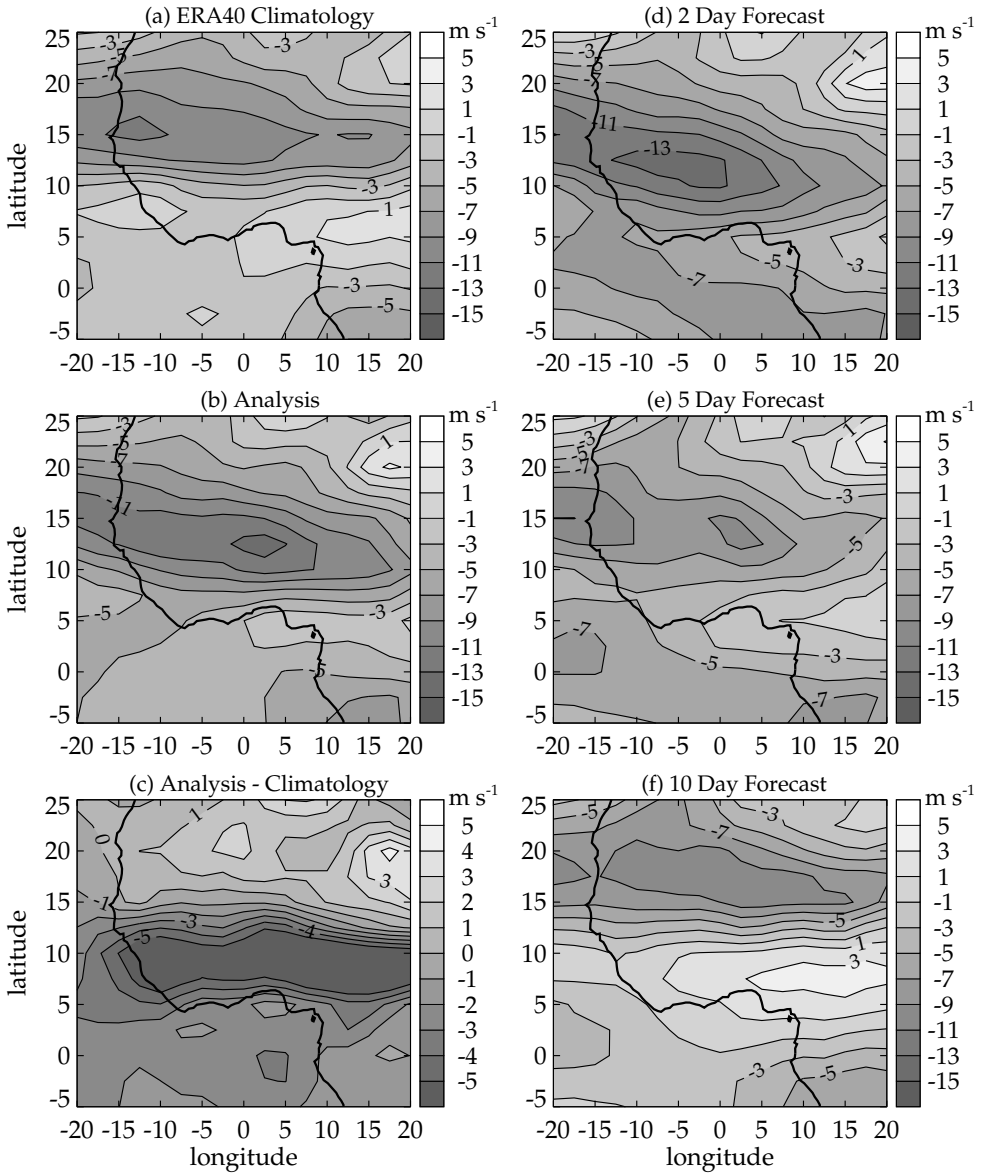

Figure 1: August monthly mean 700 hPa Zonal wind for (a) 1960-2002 ERA40 climatology, (b) August 2000 Operational Analysis, (c) anomaly (August 2000 analysis difference to climatology) (d) August 2000 2 day forecast (e) August 2000 5 day forecast (f) August 2000 10 day forecast

differences found between the model climatology and the model analyses over longer period of time, then it is possible to have confidence that conclusions drawn concerning analysis biases are more broadly applicable. To this end, fig. 1 also shows the Aug 2000 monthly mean operational forecast for ranges of 2, 5 and 10 days. Relative to the analysis, it is seen that the jet gradually weakens throughout the forecast range and migrates northwards. Examination of the intermediate forecast ranges (not shown) reveals that an approximate equilibrium is attained around day 7 to 8, thus the day 10 picture represents the model 'climatology' for this region at this time of year. The jet easterlies settle to around 10 m s^{-1}, far weaker than the analysis and the structure is very zonal. The westerlies to the south are strong, with winds approaching the same order of magnitude as the AEJ. These features of a weak jet in the medium-range agree with the previous study by Kamga et al. (2000) using an earlier version of the ECMWF system.

1.4 Overview

This paper assesses the quality of the ECMWF analyses of the AEJ and WAM system against the observations from JET2000. This represents the first time that a detailed synoptic validation of the model, albeit over limited ranges of latitude and longitude, has been possible in this region, notably in the northern Sahel and in the boundary layer. The second aim of this paper is to examine in more detail the impact of the inclusion of the high resolution dropsonde data has on this performance. Finally, the paper aims to explore the significance of different routine observational data streams in the model analyses over this region. An obvious complementary task would be the assessment of the IFS forecast capability, which is the focus of Tompkins and Jung (2005).

Section 2 gives a brief description of the operational ECMWF system as it stood at August 2000, the analysis system and the different routine observations used. Section 3 examines the quality of the ECMWF analysis using the dropsondes as a validation tool while section 4 performs the data denial studies. The final section draws the conclusions.

2 Model and methodology

2.1 Analysis system description

The ECMWF system uses a four dimensional variational analysis (4DVAR) approach which determines the model trajectory that minimizes the differences to the observations over a specific time window (e.g. Rabier et al., 1998). The system version used in this work was operational from 27th June 2000 until 12th September 2000. A 6 hour 4DVAR assimilation window was used at this time (which has since been extended to 12 hours).

In order to perform the minimization process, the tangent linear approximation of the forecast model is required, for which an exact adjoint is also necessary. The operational 4DVAR system attempts to include a formalization of relevant adiabatic and diabatic physical processes represented in the full non-linear model (e.g. Janisková et al., 1999; Mahfouf and Rabier, 2000). Note that the version of the system used in this work, operational during August 2000, included only a limited set of linearized physics in the 4DVAR system, encompassing radiative fluxes, vertical turbulent diffusion, orographic gravity waves, deep convection, and stratiform precipitation fluxes. The radiation, convection and stratiform cloud schemes have been more recently updated in two stages by Janisková et al. (2002) initially, and then by Lopez (2004) and Tompkins and Janisková (2004).

The main data that were assimilated operationally into the ECMWF analysis system during the JET2000 period are presented in table 1. Over land, the observations relate to conventional upper-air data, surface data, radiances from NOAA satellite and atmospheric motion vectors (AMVs) derived from geostationary satellite images. Figure 2 shows the distribution of conventional upper-air and surface routine observations over North Africa for 28 August 2000.

The upper air data concern the radiosondes (temp), the commercial aircraft (airep) data and the pilot wind data (where they are not concomitant to radiosondes, otherwise they are redundant and not used). Relative to regions such as Europe, N. America or E. Asia, the upper-air network is sparse over the WAM region. Aircraft data are usually restricted to a few flights or are absent altogether due to a low traffic volume of appropriately equipped aircraft. The radiosondes network covers a narrow band in latitude (around 13°N) and many of them are launched only once a day at 1200 UTC. The upper air network is increased in spatial and temporal resolution by pilot balloon launches, albeit with more limited vertical resolution and ceiling. Crucially for West Africa, there is a dearth of upper air soundings in the upstream region of eastern Africa.

Table 1: Data assimilated into ECMWF IFS system as of August 2000 in vicinity of Africa

Field	Observational Platform
Pressure	surface synop, radiosondes, ship
Temperature	radiosondes, TOVS
Humidity	surface synop, radiosondes
Horizontal winds	radiosondes, pilot balloons, aireps, meteosat cloud tracking, scatterometer (oceans,boundary layer)
Brightness Temperatures	ATOVS/TOVS, SSM/I (oceans)

The surface data network (referred to as synop over land) appear dense in relation to the upper-air data but they present considerable gaps in central Sahel and Sahara and over the adjacent Atlantic Ocean. The only synop data assimilated into the 4DVAR system are surface pressure and relative humidity: the wind is assimilated only in low terrain in the Tropics where the relief is less than 150m or over sea points, which is not the case over the considered region. The surface temperature is not assimilated directly but some information is obtained through the hydrostatic relation. Andersson et al. (1998) show that the depth of the temperature perturbation structures depends critically on the horizontal scale of the pressure perturbation. Horizontally small-scale pressure increments influence the atmospheric thickness in the lower troposphere only, with a peak in temperature increments occurring at a height of approximately 850 hPa (with an opposite sign to the surface pressure increment). On the other hand, large-scale surface pressure increments are incorporated almost barotropically, thereby affecting thickness at all levels above, resulting in small temperature increments throughout the troposphere. For average conditions, most of the temperature increments usually occurs between 850 and 700 hPa, at and below the level of the AEJ. Andersson et al. (1998) also noted a near-zero correlation between surface pressure and

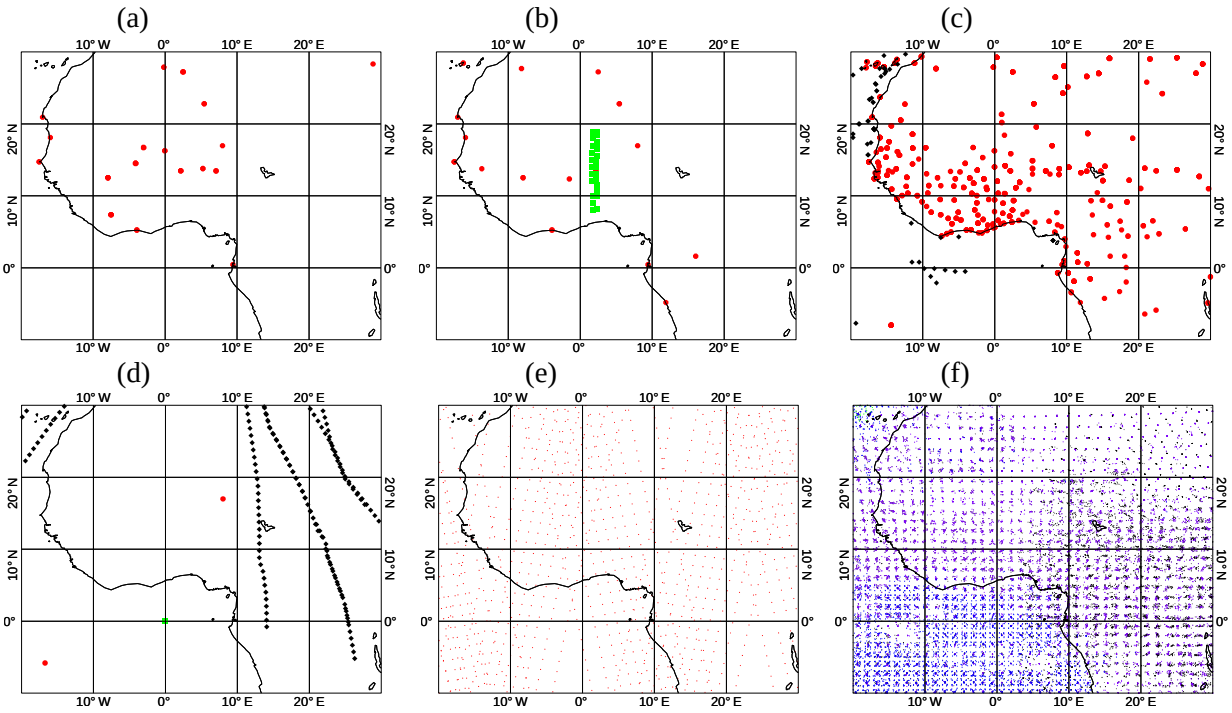

Figure 2: Location of observation assimilated into the ECMWF system on 28 August 2000. (a) Pilot balloon soundings, (b) radiosondes (circles) and dropsondes (boxes), (c) synop (circles) and ship (diamond) (d) airep (circle), amdar (diamonds) and acars (boxes), (e) ATOVS and (f) SATOB winds

temperature increments in the lowest few model levels within the planetary boundary layer (PBL).

Figure 2 also illustrates the observations of ATOVS brightness temperatures and the 'SATOB' AMV data, which for this regions is almost solely provided by the Meteosat 7 platform. The data is considerably reduced by data thinning and quality control checks. For example, the satellite brightness temperature profiles from TOVS/ATOVS vertical sounders (IR sounder, microwave sounding unit and stratospheric sounding unit) are assimilated at present only in clear sky due to the difficulty of extracting temperature and humidity information from contaminated (by cloud and precipitation) radiances. Also, the difficulties of characterising the land surface emissivity at infrared and microwave frequencies limit the use of TOVS/ATOVS radiances to the channels having no significant sensitivity to the surface. Most of the channels that provide mid to lower tropospheric information are also sensitive to the surface.

The satellite wind observations derived from geostationary images concern the VIS channel at low levels (below 700 *hPa*) and only over sea, the WV channel at high levels only (above 400 *hPa*) and the IR channel at all levels. They supply single level data at any given location, corresponding to the observed cloud top. Due to the uncertainty of the cloud being followed, this altitude assignment of the derived wind can be a significant source of error. One obvious limitation to this data source is its restriction to cloudy regions. In fact, water vapour derived AMVs are also available in clear sky regions, however, these are not currently used due to the difficulty of knowing from where in the vertical the tracked signal originates.

It is important to emphasize that the above description is valid for the ECMWF system as it stood in August 2000. Data sources, in particular satellite platforms, are always varying and the ECMWF assimilation system is continually under development in order to incorporate the new information.

2.2 Data and methodology

The ECMWF analysis system is assessed by direct comparison to the dropsonde data of temperature, relative humidity, and winds. The quoted instrumentation errors for these measurements are approximately 0.1-0.5K, 2-5%, and 0.5 m s^{-1}, respectively. The T319 (approximate 62km maximum resolution equivalent) operational system at the time successfully assimilated the dropsonde data of winds and temperature (but not humidity which is currently excluded) from the JET2000 campaign. Since this precludes their use as an independent metric for validation purposes, it was necessary to conduct a new analysis experiment for the last week of August 2000 in which all dropsonde data was rejected. The new experiment was conducted at T511 (approximate 39 km maximum resolution equivalent) horizontal resolution starting on 24 August. Apart from the improved horizontal resolution, the setup for the 4DVAR system and the model version used is identical to the operational system as of August 2000.

As described by Thorncroft et al. (2003), each flight on the 28th and 29th formed a box run in the north-south direction. For these flights, only the sondes from the longest continuous transect are used for comparison, in order to minimize the temporal disparity between the measurements. Nevertheless, the time taken for the aircraft to fly between the two extremes of the box run still exceeds 150 minutes. For each sonde, the nearest model 0.5 degree grid point to each drop location (the last position before surface impact) is identified, and all gridpoints in a transect of 5 degrees width in the cross-flight direction are averaged in order to smooth out fluctuations due to localized convective activity in the model. Since the observational data represents raw point values, it is expected to show more horizontal variability than the model fields. This is also the case with regard to vertical variability since the dropsonde data is (often) available at a superior resolution (the ECMWF system uses the current operational 60 level vertical grid). The model analysis is linearly interpolated onto a regular grid of 20 hPa resolution. The resolution of the dropsonde data can vary substantially, depending on the reporting reliability. It is thus first processed using a box-car filter with a 20hPa window size, in order that

no data is discarded when available at high resolution, and then linearly interpolated to the same 20hPa vertical regular grid for comparison to the model analysis.

3 Analysis during JET2000

3.1 North-south transects: 28 August

The analysis is first analysed for 28 and 29 August for which the C130 flew North-South transects across the Jet location. The 28 August was the focus of the preliminary investigation of Thorncroft et al. (2003). Figure 3 compares contour plots of the Zonal and Meridional winds to the T511 analysis for the first of these days. The dropsondes reveal a jet with a peak wind of 21 m s^{-1} with a tilt in the north-south direction which is sometimes characteristic of the jet structure (e.g. Cook, 1999; Nicholson and Grist, 2003; Fink et al., 2004). The jet has a broad maximum ranging from 11^oN to beyond the aircraft flight path at 8^oN. Due to the strong tilt of the jet, horizontal transects through the jet at one set altitude can portray the JET to be less extended than is actually the case, and the latitudinal location of the jet will thus also depend on the height selected for its analysis. This tilt of the Jet axis is less apparent in the analysis, which reveals a peak analysed Jet of about 16 m s^{-1}, although the averaging procedure is likely to reduce this peak figure.

Another notable contrast between the dropsonde data and the model analysis is the low level return flow. The dropsondes indicate a clear band of low level westerly flow peaking at around 4 m s^{-1}, which is almost completely absent from the model analysis. The model only supports a weak Westerly flow (around 1 m s^{-1}) northward of 14^oN. The low level flow is important for the advection of moisture from the oceans and will have a strong influence on the regional distribution of the low level equivalent potential temperature (θ_e) gradients, which in turn will affect the location and organisation of deep convection. The analysis of the low level flow should be conducted with caution however, since it is much more strongly influenced by the diurnal cycle than the wind in the free troposphere above (Racz and Smith, 1999; Parker et al., 2004a). The expectation is that deeper growth of the CBL during the day will tend to reduce the southerly and westerly components of the low level winds due to mixing-down of northeasterly momentum. The measurements at the southern most part of this leg were made at around 9am, three hours prior to the model analysis. Thus, the discrepancies between analyses and observations south of 14 N is consistent with the time lag between them.

The meridional wind is also shown in Fig. 3, and it is apparent that the model meridional wind lacks much of the fine-scale structure present in this dynamical field. The band of northerlies are too weak in the analysis and only broadly reproduce the location and structure of these winds in the dropsonde data. Moreover, the strong southerly flow at 600 hPa north of 16^oN is completely lacking in the analysis. It is possible that some of these fine-scale features in the data are the result of local deep convection, which can substantially modify the flow. The infra-red image from Meteosat 5 taken at 00 UTC on the 28th reveals substantial cirrus outflow from a deep convective convective event the previous evening exactly on the flight axis of the C130 (not shown), also noted by Taylor et al. (2003). The location of the event is just to the south of the strong southerlies in the dropsonde observations. Although the cloud signature has dissipated by the time the dropsonde measurements are made (ca. 10Z), the dynamical remnants of the system are likely to still be present.

To analyse the associated thermodynamical structure of the north-south transects, Fig. 4 shows the comparison of dropsonde temperature and relative humidity with the analysis products. Isolines mark values of the virtual potential temperature (θ_v) equal to 313 and 319 K in order to highlight the Saharan Air Layer (SAL). These are identical thresholds to those utilized by Parker et al. (2004b). In addition, an estimate for the boundary layer is given. This is calculated as the first level (starting from surface) for which θ_v exceeds the vertically integrated (from the surface to the level in question) value by 1K. The boundary layer height estimate was reasonably

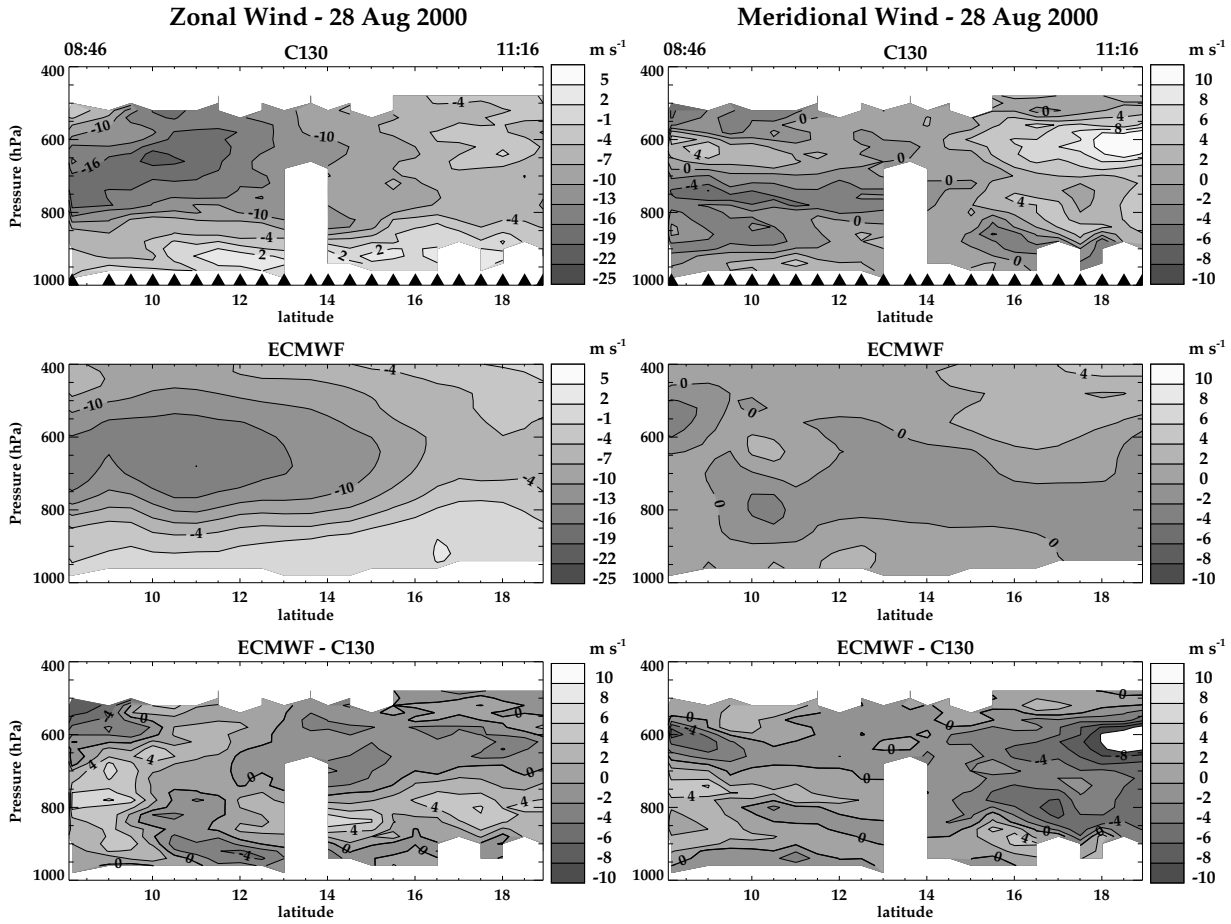

Figure 3: Comparison of dropsonde data (top) and model analysis (middle) for the zonal (left) and meridional (right) wind for 28 August 2000. The lower panels show the differences between the model and observations. For the observations the triangles at the lower border of the panel indicates the positions at which the dropsondes impacted the surface, and the two times given in the upper left and right corners state the launch time of the sondes at the transect extremes.

insensitive to this chosen threshold, although a very small value produced spatially noisy and spurious estimates with the dropsonde data.

Examining first the temperature, it is clear that above the PBL in the free troposphere, temperature errors are small in the analysis, mostly less than 1K. Considering instrumental error, the fact that the times of the dropsondes do not correspond exactly with the analysis time, and the existence of a significant north-south gradient in the tropospheric temperatures, the limited magnitude of these errors is very encouraging. The errors appear to be much larger near and within the PBL, however. A clear dipole structure is present in the analysis error field, with the model up to 4K too warm near the surface, while a significant cold bias exists above this. This would indicate a problem with the model boundary layer depth, and this is discussed further later in this section.

The relative humidity transect reveals an interesting structure in the data. To the south near the intertropical convergence zone (ITCZ) which marked the location where the majority of deep convection occurs, the profile is moist throughout the troposphere, with a broad peak exceeding 80% relative humidity at 600 to 700 hPa.

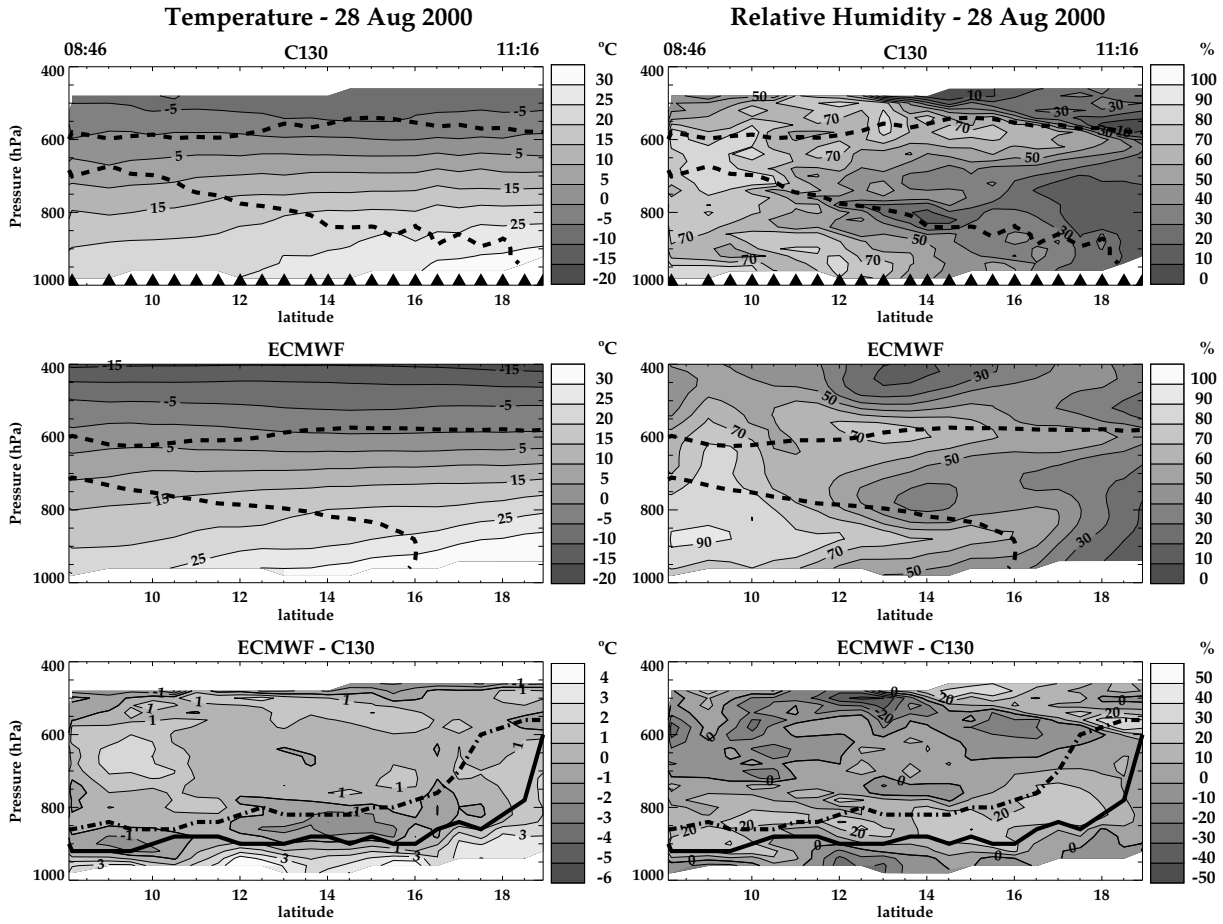

Figure 4: As Fig. 3, but for temperature (left) and relative humidity (right). On the top and middle panels, the two thick dashed lines represent the 313 and 319 K isotherms of θ_v to identify the SAL. On the lower panel the thick solid and dot-dash lines mark the estimated boundary layer height for the observations and model, respectively (see text for details of calculation).

Further north, the profile can be divided into three distinct layers. There is a clear convective outflow layer identified by high humidity, centred at about 500hPa. The upper boundary of this moist layer is extremely sharp, with the relative humidity dropping from over 50% to less than 10%. The high humidity tongue traverses the upper boundary of the SAL, as defined by the 319 K θ_v isopleth. A second moist layer exists close to the surface, where the ageostrophic direct monsoon flow advects air from over the Gulf of Guinea towards the Sahara region. Between these two moist layers a mid-level dry layer is sandwiched, between around 700 and 800 hPa, where dry Saharan air is advected southwards in the mean (see Parker et al., 2004b, for further discussion).

The model analysis of humidity provides a much smoother version of the observations, but the gross features are reasonably well represented. The 500 hPa moist outflow layer is too low in altitude and does not reproduce the orientation in the observations.

At first glance, the tongue of too high relative humidities in the analysis at roughly 900 to 850 hPa seems to indicate a too strong net advection to the north. Indeed, the same bias noted in a direct comparison of the

model analysis with low-level flight measurements was interpreted in the same way by Thorncroft et al. (2003). However, closer examination shows that the tongue of high relative humidity at ca. 900 hPa is instead associated with the boundary layer problems, and mirrors the temperature bias dipole structure, with opposing dry biases near the surface. Indeed, if the 313 K θ_v isopleth is deemed a reliable estimate of the monsoon layer low level flow, then the northward extent of this layer in the data actually surpasses that of the model analysis[1].

If one examines the near surface model errors there is a clear correlation between temperature and humidity errors, with two marked regions of warm and dry biases centred at 12 and 15^o north. It is interesting that the northern-most of these two regions coincides with the analysis of a wetted patch in the observations by Taylor et al. (2003), who pointed out that the localized wetting by precipitation the previous day causes the near surface boundary layer to be moistened, cooled and is consequently also shallower. Although it is unreasonable to expect this fine-scale structure to be reproduced in the analysis in this data-sparse region it is likely to be important that models used for medium and longer range forecasts can at least reproduce the climatology of these events.

3.2 North-south transects: 29 August

The dropsonde transects for 29 August show the very clear effect of a developing convective system at 11N. In the zonal wind (Fig. 5), an obvious acceleration of the flow between 900 hPa and the jet level provides evidence of vertical momentum transport by the convective event. The entrainment/detrainment profile of the MCS is beautifully demonstrated in the meridional wind measurements, with strong entrainment occurring between 900 and 700 hPa and detrainment above in the jet region. Since the MCS is absent from the model, the meridional wind error is dominated by this convective signal (not shown). Probably also due to the lack of the convection in the model, the zonal wind representation in the analysis is deteriorated relative to the 28th, with the model jet maximum located too far south.

The observed thermodynamic fields (Fig. 6) show the cooling and moistening of the boundary layer due to the evaporation of rainfall in the sub-cloud layer, with drying occurring above. The MCS greatly suppresses the diagnosed PBL depth as expected. Above the boundary layer the presence of the MCS greatly complicates the humidity structure, with dry regions surrounding the event between 800 and 700 hPa, presumably associated with the increased subsidence. Note the penetration of the dry tongue at 500 hPa to the vicinity of the MCS. Overall the structure resembles that described by Zipser (1977). The model is unable to reproduce the temperature and humidity structures associated with the MCS, but is able to represent the gross features northward of 12^oN with reasonable fidelity (not shown).

One issue this raises is whether the location of such MCS systems is inherently predictable, especially in a large-scale model that must rely on parametrizations to represent convective motions and small scale thermodynamical and dynamical variability. While optimal interpolation and variational analysis schemes have been used with some success to now-cast convective systems with high resolution models (e.g. Ducrocq et al., 2000; Montmerle et al., 2001), it is not certain this is achievable with model resolution of O(100km). This has implications for the generality of short-term validation exercises that are discussed further in the conclusions.

3.3 East/west transects

A significant proportion of the dropsonde wind data for the first east-west transect on 25 August was degraded, thus the final flight on 30 August is briefly examined in terms of the structure in the meridional winds. Although

[1]This is not to claim that an over-strong northward monsoon flow is not problematic in the model forecasts, explaining the error growth at the 5 day range noted by Thorncroft et al. (2003). This is also supported by examination of operation forecasts.

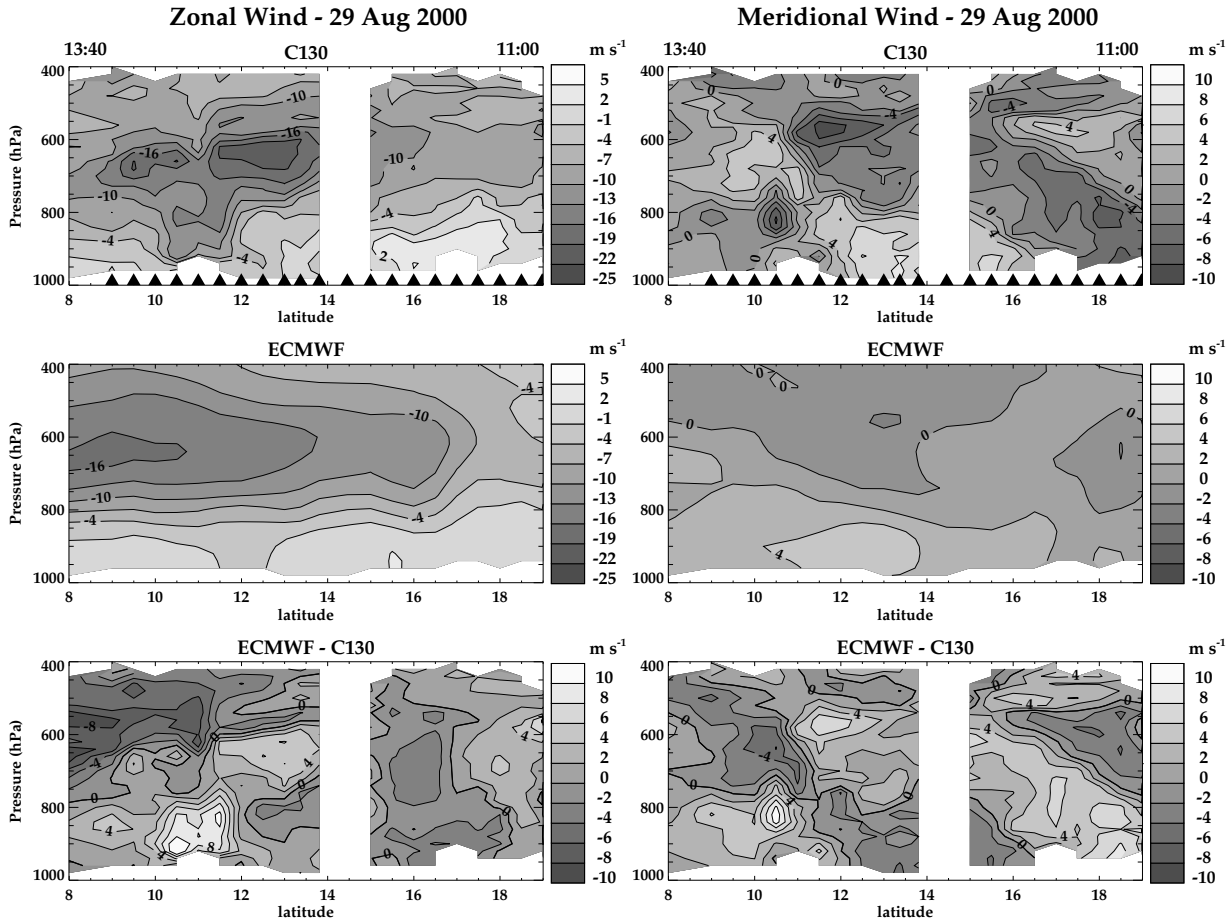

Figure 5: As Fig. 3, but for 29 August 2000

the experimental period was one not marked by strong synoptic wave activity (Thorncroft et al., 2003), a weak AEW did pass through the region on and after 29 August. This can be seen when the transect of meridional winds is examined in Fig. 7. The figure also shows the comparison to the default model analysis and it is clear that the analysis represents a wave structure, although it fails to correctly locate the peak winds, both in altitude and longitude, and which are also substantially weaker in the model.

The representation of the AEW structure is important, since systematic failure of the model in this regard could have ramifications for the ability to locate mesoscale convective systems in the short range forecasts that ultimately depend on the AEW associated wind shear and vertical stability (e.g. Grist and Nicholson, 2001). That the model is able to at least represent the gross features of this AEW reasonably well should be viewed as encouraging.

3.4 Boundary layer

In the analysis of the temperature and relative humidity errors for 28 August (Fig. 4) a dipole error structure was noted, possibly indicative of the model producing a too deep boundary layer compared to the observations on this day. Indeed, an examination of the boundary layer height estimates would appear to confirm this, with

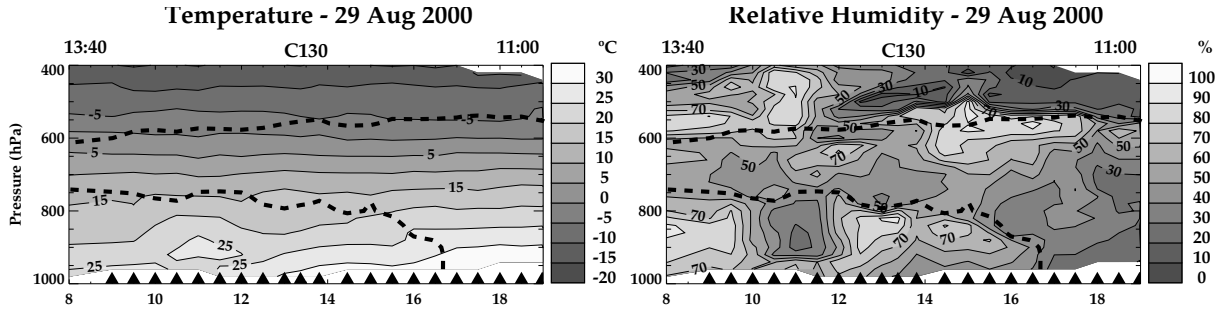

Figure 6: Dropsonde temperature (left) and relative humidity (right) with SAL layer marked as in Fig. 4

the model producing a boundary layer that is almost twice as deep as observed, and the bias dipole structure neatly demarked by the boundary layer depth estimates.

As with the PBL winds, one caveat could be the different timing of the observations, especially since the boundary layer height undergoes a strong diurnal variation in these regions. The first dropsonde in this transect was launched at 08:46 UTC while the dropsonde at the furthest north point fell approximately 2.5 hours later at 11:16Z. That said, this disparity may not provide the full explanation for the bias due to its uniformity throughout the transect. Instead one would expect a larger bias to the south where the difference in time to the analysis is greatest.

To examine this further, Fig. 8 shows the temperature error structure for the other three dates. Interestingly, it reveals the same bias structure during the west-east return flight on 30 August, while it is absent for the flights on the 25th and 29th (with the exception of the convective downdraught signal noted above).

The two east-west transects on 25 and 30 August were conducted at approximately the same time, from 10.05 to 14.51 UTC for the former, and between 10.44 and 15.15 UTC for the latter. The fact that the boundary temperature error is present through the transect on the 30th and not the 25th, and that both transects are approximately centred on the 12 UTC analysis time, implies that the the dipole error on 28 and 30 August is not an artifact of different timing between model and observations.

On 30 August, the model analysis appears to produce a boundary layer that is too deep compared to the dropsondes, in agreement with the analysis on the 28th. In contrast, the model and observed PBL depths agree very well for the 25th, when the error is absent. Close comparison of the 25th and 30th indicates that the PBL depth in the model is almost identical on these two dates. In reality the boundary layer is much shallower on the 30th, despite the slightly later timing of the dropsondes. This would suggest that the model analysis is unable to capture the day to day variation in the PBL structure. The transects of the 28th and 29th confirm this

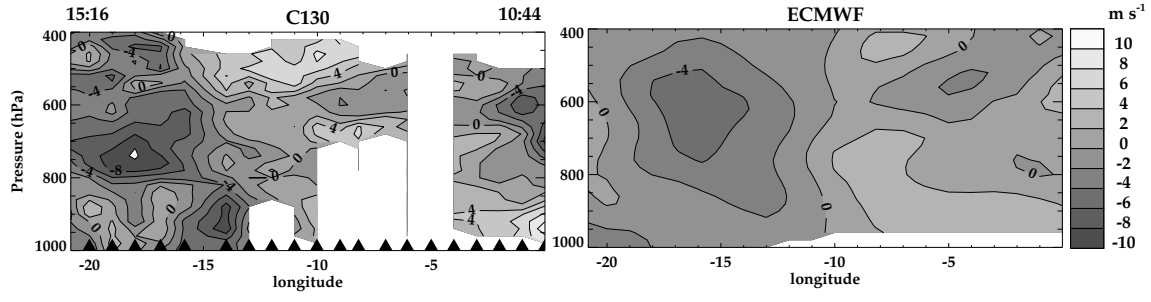

Figure 7: Dropsonde (left) and model analysis (right) meridional wind for east west flight on 30 August

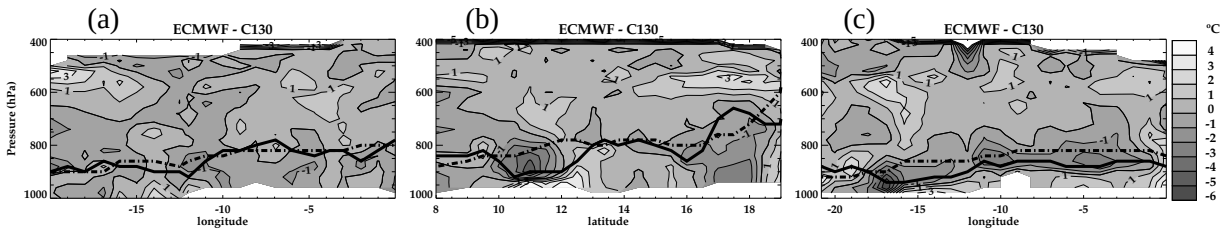

Figure 8: Differences between model analysis and dropsonde observed temperature for (a) 25, (b) 29 and (c) 30 August. The thick solid and dot-dash lines mark the estimated boundary layer height for the observations and model, respectively, as in Fig. 4 .

interpretation (compare Figs. 4 and 8). For example, between 13 and 17^{o}N on the 29th the model PBL top is around 800 hPa, in agreement with the dropsonde data. On the 28th, the model produces a slightly lower, but very similar boundary layer height between these latitudes, while the dropsondes indicate a much shallow PBL depth.

What could be causing the day to day variation in the PBL depth that the model is unable to capture? One candidate could be again deep convective systems. These can produce strong downdraughts, injecting midtropospheric low equivalent potential temperature air into the boundary layer, that could suppress its development on the following day. However, the large horizontal scale and uniformity of the bias on the days it occurs indicates that this is not the case.

Instead, it is likely that the growth in the boundary layer is affected by the thermodynamic properties of the underlying surface. Moreover, since the model is able to predict the boundary layer depth accurately for two of the four days, it is unlikely that the surface saturation (soil moisture) is at fault, since this adjusts over much slower time-scales. This suggests that the surface temperature is the cause. In fact, one of the persistent deficiencies in the analysis and medium range forecasts in this region is a lack of clouds when compared to the SYNOP reports. The model very often has clear skies over north-eastern part of the Sahel, while the SYNOP observations report large cloud fractional cover. Figure 9 shows that the model can have monthly mean cloud cover biases exceeding 4 octaves at some stations at 18 UTC (with the error maximized at 18 and 00 UTC after the mid afternoon diurnal peak in deep convection). Analysis of meteosat images (not shown) indicates that this is high cloud, generated by deep convection locally or to the south and advected northwards. The downwelling solar radiation at the surface will be too large in the model due to the lack of these clouds, warming the surface too rapidly and driving a too deep boundary layer. On clear sky days, when these clouds are absent, the model and drop sondes agree. The near ubiquitous clear sky conditions in the model explain why the boundary layer development is so uniform from day to day in the model. This serves as a warning when developing parametrization schemes, since the first impulse on diagnosing a boundary layer depth problem is to search for improvements to the vertical diffusion scheme. This analysis indicates that for this region, the problem is remotely generated, and would instead benefit from improvements to the convection and stratiform cloud parametrizations.

4 Effect of data on jet structure.

From the previous section it is clear that, despite the relative dearth of conventional data in this region and the unusual southward displacement of the jet, the analysis of the its structure for this period is quite reasonable on 28 August, in terms of strength, location, and thermodynamic properties. This section therefore attempts to ascertain which data sources are responsible for this quality of the jet analysis despite inadequacies in the model climatology in this region illustrated in the introduction.

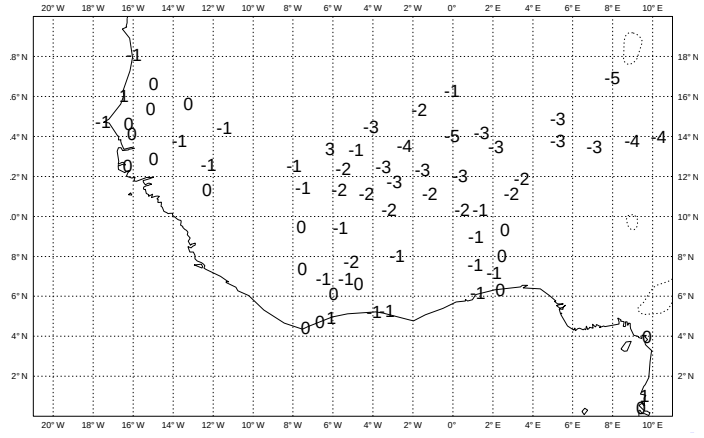

Figure 9: August 2000 monthly means cloud cover bias in Oktas, comparing the operational analysis to the Synop observations at 18Z

4.1 Denial experiments

To ascertain the importance of each standard assimilated data source, the model analysis system is rerun for the period between 23 and 30 August with each observational platform inhibited in turn. The experiments were initialized 5 days before the 28th since this is almost the 7 to 8 day period required for the model to achieve its climatology in this region and "forget" the initial state (see Fig. 1), while it is short enough to allow a wide range of sensitivity experiments to be conducted.

The details of which data sources are inhibited are given in table 2. For some of the data sources, twin experiments are conducted in which the data source is denied locally to the Sahel region in one and globally in the second. This is intended to measure the impact of the specific data source due to remote influence, for example upstream of the jet flow. The locally region spans from 0N to 30N and from 30W to 60E. Thus even the local region rejects data quite far upstream from the JET2000 dropsonde locations.

For each instrument, all quantities measured are inhibited. So for example, when radiosondes data is rejected, information concerning winds, temperature and humidity is lost to the system. Due to the computational demand required by these high resolution experiments no attempt was made to inhibit separate information sources separately for each instrument. Additionally, AIREP data is denied simultaneously with radiosondes, since it represents a similar direct in situ measurement. It was not deemed necessary to conduct a separate experiment since at most only one or two aircraft report from this region each day (cf. figure 2). However, one additional experiment attempts to partially address the issue of whether directly measured winds are more important for the jet analysis than thermodynamic information by denying all direct wind information to the system from all instruments.

Table 2: Data denial experiments conducted. 'Local' implies the region 0 to 30N and from 30W to 60E

Experiment	Data denied	region
1	radiosonde, pilot and airep	locally
2	radiosonde, pilot and airep	globally
3	Satellite	locally
4	Surface Synop and drift sondes	locally
5	All wind information	locally

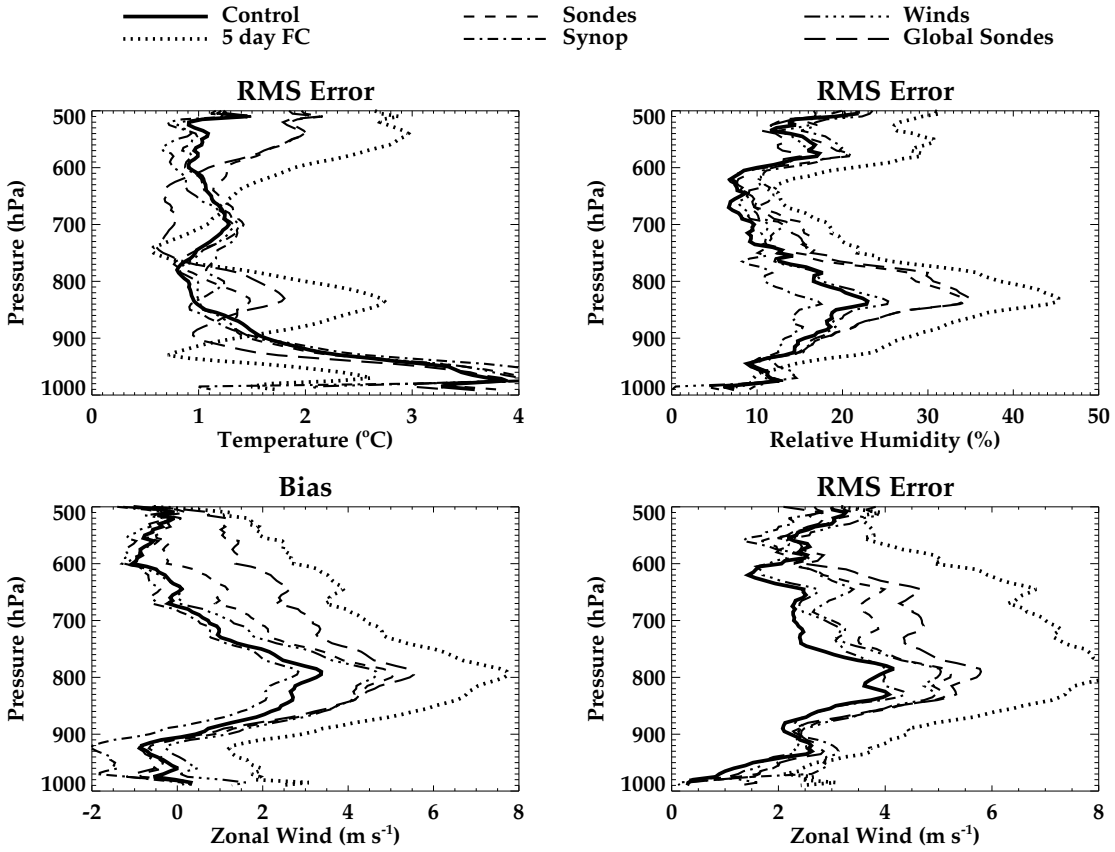

Figure 10: temperature RMS, relative humidity RMS, zonal wind mean bias and zonal wind RMS, errors for a subset of the denial experiments. See legend and main text for details.

For 28 August, the mean bias and RMS errors for temperature, relative humidity and zonal wind for the region spanning between 8N to 19N are presented in Fig. 10 for a subset of experiments. The RMS biases for the 29th were dominated by the lack of the MCS system in all analyses, resulting in similar error structures for most experiments, and thus are not shown. To place the denial experience into context, the bias and RMS errors are also given for the 5 day forecast, which are seen to be significantly greater than the analysis on 28 August.

For the zonal wind, the analysis of the jet is deteriorated when various sources of information are removed from the system. The exception is the removal of satellite data, which, while reducing the peak winds slightly, had a relatively minor effect overall and is thus not included in the figure for clarity. In each case the vertical structure is similar with the maximum of the bias and RMS errors occurring in the layer between 700 and 900 hPa.

The dominant source of information is revealed to be the collective group of radiosondes, pilot balloons and aireps, although the latter were extremely sparse and are unlikely to contribute greatly. In terms of mean bias and RMS error, neglecting these data sources over the locally defined region results in a deterioration of the zonal wind analysis that is roughly half that of the 5 day forecast at the AEJ level. This deterioration far exceeds that which results from neglecting all local wind information (the triple-dot-dash line), proving that the modification of the thermodynamic information by the radiosondes dominates the direct dynamical information. The sonde data has a significant non-local influence, witnessed by the further degradation of the jet structure when the sonde data is denied globally for this assimilation period. The relative humidity is also

deteriorated by roughly half compared to the 5 day forecast throughout the troposphere, although in this case, the radiosondes have the most impact locally, as expected.

In addition to the prevalence of the balloon soundings, Fig. 10 also indicates that the removal of surface SYNOP data appears to reduce the zonal wind mean bias throughout much of the troposphere, with an associated decline in the RMS humidity errors. This reduction in zonal wind mean bias is not associated with reduced RMS errors, which will be discussed further below.

Another artifact that deserves comment is the fact that the RMS temperature errors below 900 hPa are far smaller in the 5 day forecast than they are in the analysis. Since this is also true (albeit to a smaller degree) for 29 and 30 August (not shown), it suggests that the boundary layer problem is possibly symptomatic of the simplified physics used in the assimilation system rather than being a feature of the more complex model physics used in the forecast integrations and the assimilation trajectory calculation. The fact that none of the denial experiments appears to correct the boundary layer error to match the 5 day forecast indicates that it is not related to observations. Above the boundary layer the RMS temperature errors are mostly limited in magnitude and it is difficult to draw clear conclusions.

Overall, comparing to the 5 day forecast, which effectively designates the error resulting from the neglect of *all* data, shows that no one data source is dominant. In each case, removing one source of information is not sufficient to degrade the jet analysis to the level of the 5 day forecast; the remaining data is able to effectively constrain the system. This is an encouraging result since it indicates that the analysis system is operating as intended, with various data sources being incorporated in a well balanced manner, rather than the analysis being dominated by one data source only, despite the predominance of radiosonde information. Moreover, the balance exists not only between various observational platforms, but the continuing existence of a well formed jet when all local winds are denied to the system indicates that the analysis system is able to make a balanced use of both dynamical and thermodynamical information. One of the advantages of the 4DVAR analysis system is that altering the thermodynamic structure of the atmosphere can influence the dynamical analysis through geostrophic adjustments.

Having ascertained that the analysis systems seems to be in good balance two cases are examined in further detail: the denial of radiosonde data and SYNOP surface data, respectively. The radiosonde case is selected since its removal produced the most significant deterioration in the jet analysis. The cross section of zonal wind (Fig. 11) indicates that even for this worst case scenario, the analysis still produces a distinct jet, with the peak winds centred around 600hPa. However, it is clear that the jet core has weakened, with peak winds of 14.3 m s^{-1}, nearly 7 m s^{-1} less than observed, and the structure of jet lacks the slanted structure. Additionally, the jet core has moved too far north, producing wind errors exceeding 10 m s^{-1} at 9N. It is noteworthy that these features of a weak jet that is too far north for this longitude reproduce the climatological errors in the monthly mean forecasts, indicating that this sensitivity to radiosonde and pilot data is not specific to this particular date.

In contrast to the other data, the removal of SYNOP surface humidity and pressure data from the system appeared to be beneficial. Figure 11 reveals a jet structure in better agreement with the dropsonde data, with peak winds strengthened to 17.8 m s^{-1}, and with the slope of the jet reproduced well. In this case, the most significant error occurs at the northern most end of the flight leg, where the analysis retains an appreciable vertical winds shear between 900 and 600 hPa, which is almost absent in the data between 16 and 19 N (refer to Fig. 3). The strengthened jet is also slightly misplaced in height, being slightly lower than observed. This explains the increase in zonal wind RMS error, since for this metric, misplacing a feature such as the AEJ produces greater errors than not predicting it at all.

It is not clear from the synop denial experiment if the humidity or pressure data plays the most significant role in deteriorating the jet analysis. One would expect the pressure information to be important through its temperature impact via the hydrostatic relation and the ensuing effect on winds through geostrophic adjustment.

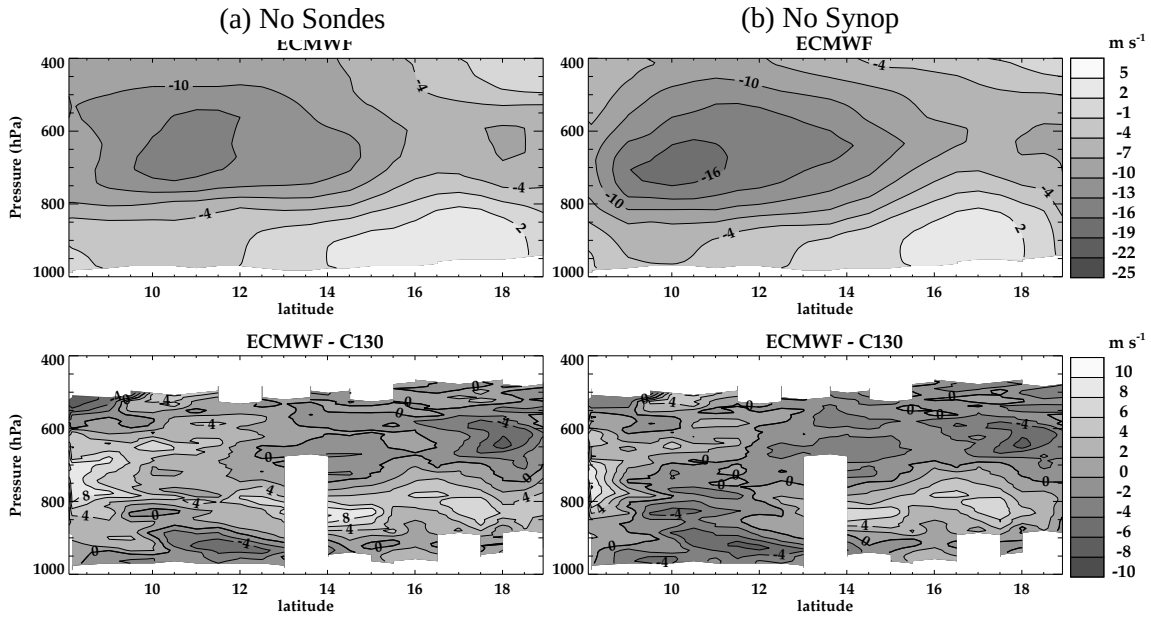

Figure 11: Zonal wind (upper) analysis and (lower) analysis differences compared to dropsonde data with specific data denied to the analysis system, namely: (a) radiosonde, pilot balloons and aircraft data or (b) synop data.

However, surface pressure can be accurately measured and it is representative of the whole vertical column (i.e. thickness). On the other hand, the humidity information available from SYNOP stations has been shown to conflict with low level radiosonde (and in this campaign, dropsonde) data. The low level humidity is also vital for the jet structure since it is the central determinant of low level moist static energy which influences the location of deep convection. Moreover, the assimilation system tends to spread out the information in the vertical through the vertical structure functions, whereas it is not always clear if humidity measurements taken at a height of 2m are representative of the deeper atmosphere or can render useful information above the boundary layer, especially at night[2]. It is for these reasons that many forecast models choose not to assimilate synop humidity information. It is thus likely that it is the SYNOP humidity information that causes the deterioration of the jet structure.

In summary, this section shows that radiosonde data dominates the model analysis through the thermodynamic information provided. Although dominant, the data assimilation is able to effectively combine all data sources in a balanced way, such that removal of any one data source does not produce the model climatology.

4.2 Effect of dropsonde data

The sensitivity of the analysis to the addition of the dropsonde data is examined. The last section documented a strong reliance on the conventional soundings in this region. The radiosonde and pilot ascents provide isolated measurements of the atmospheric state that are sparse, but sample a wide geographical area. The issue raised here is whether more useful information is obtained by supplementing this with the dense dropsonde data which covers a narrow region directly in the vicinity of the JET axis.

The use of the dropsonde data in the analysis negates their status as an independent data source for verification, however, it is still a valuable exercise to see if the assimilation is able to incorporate this information in a well

[2]In fact, the latest version of the ECMWF analysis system implemented in September 2004 excludes SYNOP humidity information at night.

Date	Range	data	Peak -U m s^{-1}	-U m s^{-1}	T K	RH %
28th	Dropsonde observations		21.2	7.4	12.3	52
28th	Analysis	- drops	16.1	6.5	13.0	57
28th	Analysis	+ drops	18.3	7.3	12.2	52
29th	Dropsonde observations		21.0	7.3	12.5	53
29th	Analysis	- drops	17.1	6.7	12.7	64
29th	Analysis	+ drops	16.5	7.3	13.0	52
30th	Dropsonde observations		22.0	10.3	11.7	59
30th	Analysis	- drops	15.5	7.9	12.1	62
30th	Analysis	+ drops	18.1	8.9	12.2	59

balanced fashion, and to what spatial extent the high resolution data has an impact. (Additionally, it is possible to examine the temporal impact, in other words, the effect the sonde information has on the short and medium range forecast of the AEJ, which is the focus of Tompkins and Jung, 2005).

The mean values of zonal wind, temperature and relative humidity across the transect for 28, 29 and 30 August are given in table 3, along with the peak zonal wind. The table indicates that the additional dropsonde data is successfully assimilated and with the model analysis drawing closer to the observations in most quantities. For example, the easterly mean wind is very close to the dropsonde data for the first two days and draws nearer for the 30th. The peak winds are also improved on the 28th and 30th, although a small deterioration is noted on the 29th. Results are mixed for temperature, possibly due to the boundary layer problem pointed out earlier, while the humidity information appears to be effectively assimilated, with the relative humidity almost perfect when dropsonde data is used[3].

The full impact of the sondes on the analyses of the jet can be seen in 12. If the revised analyses are compared to the corresponding observations and default analyses in Figs. 3 and 5, it is clear that the dropsonde data improves the location, structure, tilt and northerly extent of the jet diagnosis.

5 Conclusions

The African easterly jet is one of the key elements of the West African Monsoon system, which is a major climatic feature of sub-Saharan North Africa, one of the most densely populated regions of the African continent, and has important impacts on the tropical North Atlantic. Its analysis and forecast in weather centre models is therefore critical.

During August 2000, the Met Office C130 research flight aircraft conducted four sorties over the Western Sahel region, taking measurements in the vicinity of the jet of humidity, temperature and winds, using dropsondes at an unprecedented horizontal resolution. These measurements were used in two ways. Firstly, using the ECMWF integrated forecast system model at T511 horizontal resolution, the dropsonde data were used as an independent validation source to assess the quality of the ECMWF analysis of the JET. The model was found to produce a reasonably accurate representation of the jet location and structure despite its displacement to the south relative to climatology. Peak zonal winds were within 5 ms^{-1} of the observed values for the two flight performed transects across the jet, and temperature errors were limited to less than 3 K, and mostly 1K above the boundary layer. The humidity structure also resembled the data, with a dry mid-tropospheric tongue

[3]note that this version of the model does not use the revised RH based control variable introduced into the ECMWF 4DVAR system (Holm et al., 2002) and the temperature biases imply small humidity biases still remain.

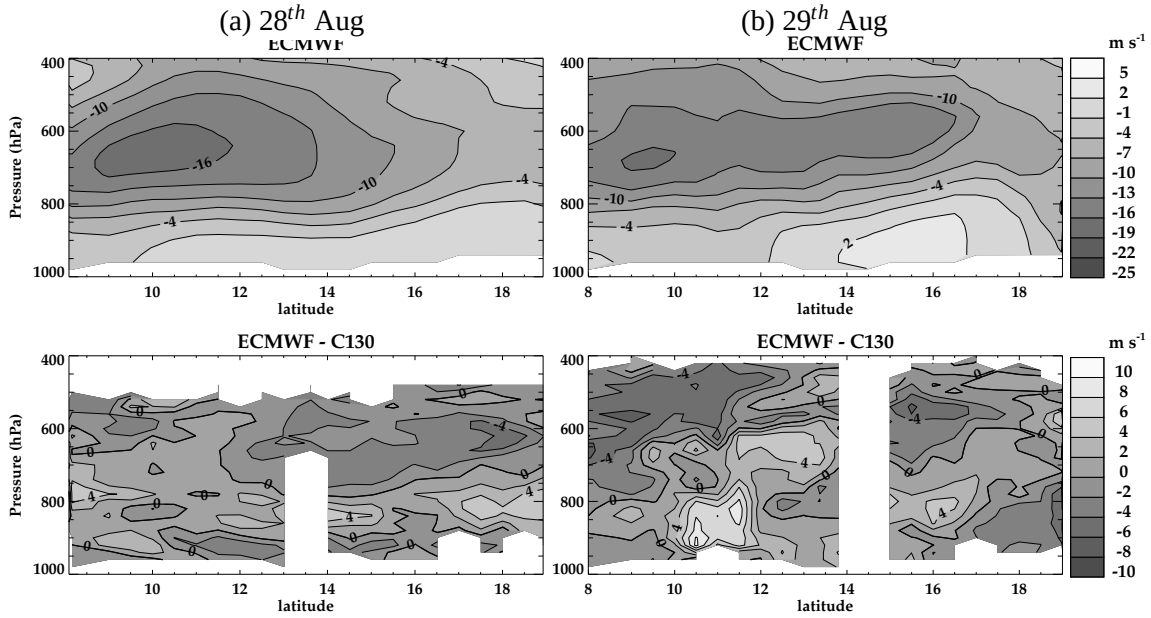

Figure 12: Zonal wind analysis and analysis differences to dropsonde data when dropsonde data is assimilated for (a) 28 August and (b) 29 August. Refer to Figures. 3 and 5 for dropsonde data.

sandwiched between two moist layers associated with deep convective outflow to the south and the low level monsoon flow.

In terms of the meridional winds, the data revealed the passage of a weak Easterly wave during the campaign, which was also captured by the model analysis. The model wave was slightly weaker and displaced eastwards relative to the observations. On two occasions the diagnosed boundary layer depth was too deep, with a clear bimodal structure in the temperature and relative humidity errors. This was apparently linked to an inability to diagnose the daily variations in boundary layer depth. The days in which model was incorrect were marked by a shallow boundary in the dropsonde observations. It is suggested that the near ubiquitous clear sky conditions in the model are to blame, with the absence of the high level cloud often observed in the region allowing too much solar radiation to reach the surface in these regions.

The study then examined which data sources were important for the prediction of the jet in the analysis. A series of analysis experiments were conducted in which various data platform were excluded from the system for a sizable local region starting over the Atlantic at 30W, spanning the Sahel to 60E. It was found that the use of Satellite data for this region had only a minor effect on the jet structure. In contrast, data from conventional platforms such as radiosondes and pilot balloons (which only provide information concerning the vertical wind profile) were more important. An additional experiment in which local wind information from all platforms was denied from the system indicated that the thermodynamical information from radiosondes has a greater impact on the analysis winds through the thermal wind balance equation, than the direct assimilation of wind data itself. A significant non-local influence was identified since the removal of radiosondes globally produced a further deterioration of the jet analysis. Notably, some (but not all) characteristics of the jet region, such as peak jet winds and the mid tropospheric zonal wind biases, were actually improved when SYNOP surface station information was removed from the system. The most likely cause is the apparent disparity between the radiosonde and SYNOP station humidity information over these regions, with the SYNOP measurements being at times up to 2 g kg^{-1} moister than the former. The low level humidity is the primary predictor for moist static energy and therefore CAPE and strongly influences the location and occurrence of deep convection.

Encouragingly, none of the denial experiments revealed a deterioration of the jet structure to the level of the 5 day forecast for 28 August. This indicates that the analysis system is performing as intended and using all observational information in a well balanced manner, rather than being dominated by a sole source.

Finally, the study attempted to ascertain the effect of adding the dropsondes information to the analysis system. Of course, the assimilation of the dropsondes precludes their independent status for model validation. However, it is important to ascertain if the 4DVAR system is able to assimilate this high resolution data source successfully in this data sparse region. The study showed this was indeed the case, with the data improving the structure of the analysis. Although of high spatial resolution, the dropsondes only cover a limited geographical extent, and the analysis was only impacted locally by their incorporation, most notably in the relative humidity field. A natural progression would be to investigate if the dropsondes have a positive impact on the short-range forecasts, and this is the focus of Tompkins and Jung (2005).

While this work reveals some interesting strengths and shortcomings of the ECMWF system, one possible caveat discussed in the introduction is the limited nature of the observations, both in time and space. With only two days of transects taken through the jet, one may reasonably question the generality of the findings. The presence of mesoscale convective events may locally alter the jet thermodynamic and/or dynamical structure. Even if a model produces the statistics of such systems well, the inherent lack of predictability of such systems could invalidate conclusions drawn from 'snap-shot' comparisons. Indeed, the observations for 29 August reveals the signature of just such a system, missing from the model analysis. Moreover, examination of the ERA40 reanalysis for summer 2000 revealed it to be an unusual year relative to climatology with a southerly displaced jet, stronger and more zonal than usual, and undergoing no significant 'break' periods for the preceeding two months. That said, when the radiosonde data was removed from the analysis system on the 28th, the analysis errors, when compared to the independent dropsonde data, showed the same characteristics of a weakened jet displaced to the north as seen when comparing monthly mean 10 day forecasts (the model climate) to the analysis. The same errors, albeit to a lesser extent, were observed in the default analysis on both 28 and 29 August. This similarity suggests that the findings of the study have general relevance to the model.

It is emphasized that this study pertains to the model version operational in August 2000, and since this period the IFS system has continued to evolve with changes made to the physics and numerics, in addition to the analysis system and data usage. Nevertheless, the study points towards the need for further spatially and temporally intensive observations to be conducted over this region for a significant period of time, preferably spanning a number of seasons. In fact, such a project in currently under way in the form of the African Monsoon Multidisciplinary Analyses (AMMA, see http://medias.obs-mip.fr/amma/), which will provide enhanced data over this region for a number of years, allowing one to validate the preliminary findings of this study that uses the pilot JET2000 campaign. In particular, AMMA will aim to supplement more conventional thermodynamical and dynamical measurements with an array of aerosol information. One of the array of changes to the IFS system mentioned above involved the implementation of a new aerosol climatology and a companion paper (Tompkins et al., 2005) demonstrates that the direct radiative impact of this change greatly improves the representation of the African Easterly Jet, both in the analysis, and perhaps more importantly in the medium-range forecasts.

Acknowledgements

The JET2000 experiment was funded by NERC under Grant GR3/13118. C. Thorncroft has been partially funded for this work by NSF (PTAEO: 1023911- 1-24796). We would like to acknowledge the support we received at the Cape Verde and Niger Meteorological Services and thank Mr. Soares from Cape Verde and Idrissa from Niger. The support received from ACMAD in Niger, in particular Mr. Boulaya and Mr. Afiesimama,

was greatly appreciated. We would also like to acknowledge the input of the aircrew and aircraft scientists of the Meteorological Research Flight. Martin Miller is thanked for comments on this paper and Erik Andersson carefully vetted and improved the description of the ECMWF 4DVar assimilation system.

References

Andersson, E., J. Haseler, P. Unden, P. Courtier, G. Kelly, D. Vasiljevic, C. Brankovic, C. Cardinali, C. Gaffard, A. Hollingsworth, C. Jakob, P. Janssen, E. Klinker, A. Lanzinger, M. Miller, F. Rabier, A. Simmons, B. Strauss, J. Thepaut, and P. Viterbo, 1998: The ECMWF implementation of three-dimensional variational assimilation (3D-Var). III: Experimental results, *Q. J. R. Meteorol. Soc.*, **124**, 1831–1860.

Burpee, R., 1972: The origin and structure of easterly waves in the lower troposphere of North Africa, *J. Atmos. Sci.*, **29**, 77–90.

Cook, K. H., 1999: Generation of the african easterly jet and its role in determining west african precipitation, *J. Climate*, **12**, 1165–1184.

Diongue, A., J.-P. Lafore, J.-L. Redelsperger, and R. Roca, 2002: Numerical study of a sahelian synoptic weather system: Initiation and mature stages of convection and its interactions with the large-scale dynamics, *Q. J. R. Meteorol. Soc.*, **128**, 1899–1927.

Ducrocq, V., J. Lafore, J.-L. Redelsperger, and F. Orain, 2000: Initialization of a fine-scale model for convective-system prediction: A case study, *Q. J. R. Meteorol. Soc.*, **126**, 3041–3065.

Eltahir, E. A. B., 1998: A soil moisture-rainfall feedback mechanism. 1. theory and observations, *Water Resour. Res.*, **34**, 765–776.

Fink, A. H. and P. M. Reiner, 2003: Spatiotemporal variability of the relation between African Easterly Waves and West African Squall Lines in 1998 and 1999, *J. Geophys. Res.*, **108**, 4332, doi:10.1029/2002JD002816.

Fink, A. H., D. G. Vincent, P. M. Reiner, and P. Speth, 2004: Mean state and wave disturbances during Phases I, II, and III of GATE based on ERA-40, *Mon. Wea. Rev.*, **132**, 1661–1683.

Fontaine, B., N. Philippon, and P. Camberlin, 1999: An improvement of June-September rainfall forecasting in the Sahel based upon region April-May moist static energy content (1968-1997), *Geophys. Res. Lett.*, **26(14)**, 2041–2044.

Grist, J. P. and S. E. Nicholson, 2001: A study of the dynamic factors influencing the rainfall variability in the West African Sahel, *J. Climate*, **14**, 1337–1359.

Holm, E., E. Andersson, A. Beljaars, P. Lopez, J.-F. Mahfouf, A. Simmons, and J.-N. Thepaut, 2002: Assimilation and Modelling of the Hydrological Cycle: ECMWF's Status and Plans, Technical Report 383, European Centre for Medium-Range Weather Forecasts, available at http://www.ecmwf.int/publications/, pp55.

Janisková, M., J.-F. Mahfouf, J.-J. Morcrette, and F. Chevallier, 2002: Linearized radiation and cloud schemes in the ECMWF model: Development and evaluation, *Q. J. R. Meteorol. Soc.*, **128**, 1505–1527.

Janisková, M., J.-N. Thepaut, and J.-F. Geleyn, 1999: Simplified and regular physical parameterizations for incremental four-dimensional variational assimilation, *Mon. Wea. Rev.*, **127**, 26–45.

Kamga, A. F., S. Fongang, and A. Viltard, 2000: Systematic errors of the ECMWF operational model over tropical Africa, *Mon. Wea. Rev.*, **128**, 1949–1959.

Karyampudi, V. M. and T. N. Carlson, 1988: Analysis and numerical simulations of the saharan air layer and its effect on easterly wave disturbances, *J. Atmos. Sci.*, **45**, 3102–3136.

Laurent, H., N. D'Amato, and T. Lebel, 1998: How important is the contribution of the mesoscale convective complexes to the sahelian rainfall?, *Phys. Chem. Earth.*, **23**, 629–633.

Le Barbé, L., T. Lebel, and D. Tapsoba, 2002: Rainfall variability in west Africa during the years 1950-90, *J. Climate*, **15**, 187–202.

Lopez, P., 2004: A convection scheme for data assimiliation purposes: Description and initial tests, *Q. J. R. Meteorol. Soc.*, submitted.

Mahfouf, J.-F. and F. Rabier, 2000: The ECMWF operational implementation of four-dimensional variational assimilation. II: Experimental results with improved physics, *Q. J. R. Meteorol. Soc.*, **126**, 1171–1190.

Montmerle, T., A. Caya, and I. Zawadzki, 2001: Simulation of a midlatitude convective storm initialized with bistatic doppler radar data, *Mon. Wea. Rev.*, **129**, 1949–1967.

Newell, R. E. and J. W. Kidson, 1984: African mean wind changes between sahelian wet and dry periods, *Int. J. Climatol.*, **4**, 27–33.

Nicholson, S. E., 1981: Rainfall and atmospheric circulation during drought periods and wetter years in west Africa, *Mon. Wea. Rev.*, **109**, 2191–2208.

Nicholson, S. E. and J. P. Grist, 2003: The seasonal evolution of the atmospheric circulation over West Africa and equatorial Africa, *J. Climate*, **16**, 1013–1030.

Parker, D. J., R. R. Burton, A. Diongue, M. F. R. J. Ellis, C. M. Taylor, C. D. Thorncroft, and P. Bessemoulin, 2004a: The diurnal cycle of the West African Monsoon circulation, *Q. J. R. Meteorol. Soc.*, **130**, conditionally accepted.

Parker, D. J., C. Thorncroft, R. Burton, and A. Diongue-Niang, 2004b: Analysis of the African Easterly Jet using aircraft observations from the JET2000 experiment, *Q. J. R. Meteorol. Soc.*, **130**, conditionally accepted.

Rabier, F., J.-N. Thepaut, and P. Courtier, 1998: Extended assimilation and forecast experiments with a four-dimensional variational assimilation system, *Q. J. R. Meteorol. Soc.*, **124**, 1861–1887.

Racz, Z. and R. K. Smith, 1999: The dynamics of heat lows, *Q. J. R. Meteorol. Soc.*, **125**, 225–252.

Redelsperger, J.-L., A. Diongue, A. Diedhiou, J.-P. Cron, M. Diop, J.-F. Gurmy, and J.-P. Lafore, 2002: Multi-scale description of a sahelian synoptic weather system representative of the west african monsoon, *Q. J. R. Meteorol. Soc.*, **128**, 1229–1257.

Reed, R. J., A. Hollingsworth, W. A. Heckley, and F. Delsol, 1988: An evaluation of the performance of the ecmwf operational system in analyzing and forecasting easterly wave disturbances over africa and the tropical atlantic, *Mon. Wea. Rev.*, **116**, 824–865.

Simmons, A. J. and J. K. Gibson, 2000: The ERA-40 project plan, Technical Report 1, Era-40 Project Report Series, available at http://www.ecmwf.int/publications/.

Sultan, B. and S. Janicot, 2003: The west African monsoon dynamics. Part II: The "preonset" and "onset" of the summer monsoon, *J. Climate*, **16**, 3407–3427.

Sultan, B., S. Janicot, and A. Diedhiou, 2003: The west African monsoon dynamics. Part I: Documentation of intraseasonal variability, *J. Climate*, **16**, 3389–3406.

Taylor, C. M., R. J. Ellis, D. J. Parker, R. R. Burton, and C. D. Thorncroft, 2003: Linking boundary-layer variability with convection: A case-study from JET2000, *Q. J. R. Meteorol. Soc.*, **129**, 2233–2253.

Thorncroft, C. D. and M. Blackburn, 1999: Maintenance of the African easterly jet, *Q. J. R. Meteorol. Soc.*, **125**, 763–786.

Thorncroft, C. D., D. J. Parker, R. R. Burton, M. Diop, J. H. Hayers, H. Barjat, R. Dumelow, D. R. Kindred, N. M. Price, C. M. Taylor, and A. M. Tompkins, 2003: The JET2000 experiment: Aircraft observations of the African easterly jet and African easterly waves, *Bull. Amer. Meteor. Soc.*, **84**, 337–351.

Tompkins, A. M., C. Cardinali, J.-J. Morcrette, and M. Rodwell, 2005: Influence of aerosol climatology on forecasts of the African Easterly Jet, *Geophys. Res. Lett.*, submitted.

Tompkins, A. M. and M. Janisková, 2004: A cloud scheme for data assimiliation: Description and initial tests, *Q. J. R. Meteorol. Soc.*, **130**, 2495–2518.

Tompkins, A. M. and T. Jung, 2005: African easterly jet in the ECMWF integrated forecast system: forecast and sensitivity, *Q. J. R. Meteorol. Soc.*, in preparation.

Zheng, X. and E. A. B. Eltahir, 1998: The role of vegetation in the dynamics of west african monsoons, *J. Climate*, **11**, 2078–2096.

Zheng, X., E. A. B. Eltahir, and K. A. Emmanuel, 1999: A mechanism relating tropical Atlantic spring sea surface temperature and west african rainfall, *Q. J. R. Meteorol. Soc.*, **125**, 1129–1164.

Zipser, E. J., 1977: Mesoscale and convective-scale downdraughts as distinct components of squall-line circulation, *Mon. Wea. Rev.*, **105**, 1568–1589.